NASA TECHNICAL MEMORANDUM 104055
AVSCOM TECHNICAL REPORT 91-B-010

NASA-TM-104055 19910018979

LOCAL DELAMINATION IN LAMINATES WITH ANGLE PLY MATRIX CRACKS: PART I TENSION TESTS AND STRESS ANALYSIS

T. K. O'Brien, and S. J. Hooper

Paper Presented at the 4th ASTM Conference on Composite Materials: Fatigue and Fracture Indianapolis, Indiana May 6-7, 1991

JUNE 1991

National Aeronautics and Space Administration

Langley Research Center
Hampton, Virginia 23665

US ARMY AVIATION SYSTEMS COMMAND
AVIATION R&T ACTIVITY

DISPLAY 27/2/1

91N28293*# ISSUE 20 PAGE 3305 CATEGORY 24 RPT#: NASA-TM-104055 NAS 1.15:104055 AVSCOM-TR-91-B-010-PT-1 91/06/00 33 PAGES UNCLASSIFIED DOCUMENT

UTTL: Local delamination in laminates with angle ply matrix cracks. Part 1: Tension tests and stress analysis

AUTH: A/OBRIEN, T. KEVIN; B/HOOPER, S. J. PAA: B/(Wichita State Univ., KS.)

CORP: National Aeronautics and Space Administration. Langley Research Center, Hampton, VA.; Army Aviation Systems Command, Hampton, VA.

SAP: Avail: NTIS HC/MF A03

CIO: UNITED STATES Prepared in cooperation with Army Aviation Systems Command, Hampton, VA Presented at the 4th ASTM Conference on Composite Materials: Fatigue and Fracture, Indianapolis, IN, 6-7 May 1991

MAJS: /*CRACK PROPAGATION/*DELAMINATING/*GRAPHITE-EPOXY COMPOSITES/*LAMINATES/*STRESS ANALYSIS/*TENSILE TESTS/*X RAY INSPECTION

MINS: / COMPRESSIBILITY/ DAMAGE ASSESSMENT/ DYES/ FINITE ELEMENT METHOD/ PLATE THEORY/ PLATES (STRUCTURAL MEMBERS)/ TENSILE STRESS

ABA: Author

ABS: Quasi-static tension tests were conducted on AS4/3501-6 graphite epoxy laminates. Dye penetrant enhanced x-radiography was used to document the onset of matrix cracking and the onset of local delaminations at the intersection of the matrix cracks and the free edge. Edge micrographs taken after the onset of damage were used to verify the location of the

MORE

ENTER:

4B

.PRT

SUMMARY

Quasi-static tension tests were conducted on AS4/3501-6 graphite epoxy $(0_2/\theta_2/-\theta_2)_s$ laminates, where θ was 15, 20, 25, or 30 degrees. Dye penetrant enhanced X-radiography was used to document the onset of matrix cracking in the central $-\theta$ degree plies and the onset of local delaminations in the $\theta/-\theta$ interface at the intersection of the matrix cracks and the free edge. Edge micrographs taken after the onset of damage were used to verify the location of the matrix cracks and local delaminations through the laminate thickness.

A quasi-3D finite element analysis was conducted to calculate the stresses responsible for matrix cracking in the off-axis plies. Laminated plate theory indicated that the transverse normal stresses were compressive. However, the finite element analysis yielded tensile transverse normal stresses near the free edge. Matrix cracks formed in the off-axis plies near the free edge where in-plane transverse stresses were tensile and had their greatest magnitude. The influence of the matrix crack on interlaminar stresses is also discussed.

INTRODUCTION

Local delaminations that form at the intersection of matrix cracks in off-axis angle plies and the free edges of a composite laminate have been observed in unnotched, notched, and tapered laminates [1,2,3]. The accumulation of local delaminations through the laminate thickness redistributes the strain in the zero degree plies resulting in fatigue failures [4]. Previously, local delamination onset in fatigue from 45 degree matrix ply cracks was predicted using a simple closed form solution for the strain energy release rate associated with this mechanism [3,4]. However, in order to demonstrate the general applicability of this technique, local delaminations from matrix cracks of arbitrary orientation must be studied. Such solutions could then be applied to arbitrary layups, such as the ones resulting from a rotated straight edge analysis for delamination around an open hole [5], to predict fatigue life.

In this study, tension tests were conducted on $(0_2/\theta_2/-\theta_2)_s$ AS4/3501-6 graphite/epoxy laminates, where θ was 15, 20, 25, and 30 degrees. Dye penetrant enhanced X-ray radiography was used to document the onset of matrix cracking, and the onset of local delaminations at the intersection of the matrix cracks and the free edge. A quasi-3D finite element analysis was conducted to calculate the stresses responsible for matrix cracking in the off-axis plies. These stresses were compared to stresses calculated from laminated plate theory. The influence of the matrix crack on interlaminar stresses was also discussed.

EXPERIMENTS

Materials

Panels were manufactured in an autoclave at NASA Langley Research Center from Hercules AS4/3501-6 graphite epoxy prepreg using the standard manufacturer's procedure with a maximum temperature of 177°C (350°F) in the cure cycle. One panel was produced for each of the $(0_2/\theta_2/-\theta_2)_s$ layups, where θ was 15, 20, 25, or 30 degrees. Panels 305 mm (12 in.) square were manufactured and then cut into 20 individual coupons, 127 mm (5 in.) long by 25 mm (1.0 in.) wide. Each specimen had a nominal ply thickness of 0.124 mm (0.0049 in.) and a fiber volume fraction of 66.5%.

Experimental Procedure

Coupons were coated with a thin film of water-based typewriter correction fluid on either edge to act as a brittle coating for detecting the onset of matrix cracking and delamination. Then, specimens were placed in the hydraulic grips of an MTS hydraulic load frame such that each specimen had a gage length between the grips of approximately 76 mm (3.0 inches). A 25 mm (one inch) gage length extensometer was mounted on the specimen midway between the grips to measure nominal strain. Specimens were loaded in tension at a rate of 13 mm/min. (0.5 in./min). During the loading, a plot of load versus nominal strain was generated using an X-Y recorder. Specimens were loaded until the first audible indication of cracking was heard. All tests had linear load vs. nominal strain plots up to this point when the loading was stopped. The load was maintained on the specimen to enhance the ability to detect damage, but was reduced by approximately 5-10% to prevent the possibility of the formation of further damage, or damage growth due to creep. The edge was examined visually with a magnifying glass while the specimen was under load to determine if a matrix crack or delamination had formed. In addition, a zinc iodide solution that was opaque to X-rays was placed on the edge using a hypodermic needle and an X-ray photograph was taken of the specimen width. After the onset of cracking was detected, specimens were removed from the load frame and the specimen edges were polished. Photographs of the polished edges were taken through an optical microscope to examine the damage on the edge.

Experimental Results

In all cases, the radiograph taken at the first audible indication of the onset of damage showed at least one, and in some cases up to ten, matrix cracks in the central -θ degree plies (fig.1). The θ = 15 and 20 degree laminates (fig.1a&b) typically had only one or two matrix cracks, whereas the θ = 25 and 30 degree laminates (fig.1c&d) typically had two or more matrix cracks. The dark squares in the center of the laminate are thin aluminum blocks that were bonded to the specimen surface to hold the knife edges of the extensometer. The radiographs also showed a triangular-shaped shaded region bounded by the free edge and the matrix crack, indicating that a local delamination was present (fig.1). Figure 2 shows photographs of the edge of laminates that were tested under a

monotonically increasing tension load until the onset of damage. As shown in figure 2, local delaminations were present in both $\theta/-\theta$ interfaces, extending in the same direction from curved matrix cracks in the central $-\theta$ degree plies. For all the specimens tested, the radiographs and edge micrographs indicated that both the $-\theta$ degree ply matrix crack and the $\theta/-\theta$ interface delaminations were present. There was no evidence of the presence of matrix cracking without the delamination, nor was there any evidence of the presence of delamination without a matrix crack.

STRESS ANALYSIS

Laminated Plate Theory

Laminated plate theory [6] was used to calculate the in-plane stresses in the central $-\theta$ degree plies for $(0/\theta/-\theta)_s$ graphite epoxy laminates, using lamina properties listed in Table 1. The in-plane stresses were transformed into the lamina coordinate system, and the stresses normal to the fiber direction, σ_{22}, and the shear stresses along the fiber direction, τ_{12}, were determined. These stress components contribute directly to the formation of matrix ply cracks.

Figure 3 shows calculated values of σ_{22} and τ_{12} as a function of θ for $(0/\theta/-\theta)_s$ graphite laminates subjected to a total (mechanical + thermal) axial strain of 0.01, assuming a ΔT of -156°C (-280°F). This ΔT corresponds to the difference in the cure temperature of 177°C (350°F) and a room temperature of 21°C (70°F) at which the laminates were tested. These laminated plate theory results indicate that for $(0/\theta/-\theta)_s$ graphite laminates, where θ is between 15 and 30 degrees, relatively high shear stresses are present along the fiber direction but the transverse normal stresses are compressive. For $\theta > 30$ degrees, the shear stresses are also high, but the transverse normal stresses are tensile.

The stresses plotted in figure 3, that were calculated assuming a ΔT of -156°C (-280°F), correspond to laminates that are completely dry. However, the epoxy matrix will absorb moisture from the air. This absorbed moisture in the matrix creates swelling stresses in the laminate. These swelling stresses tend to relax the residual thermal stresses that result from cooling the laminate after it is cured. If enough moisture is absorbed such that the residual thermal stresses are completely relaxed, the stresses in

the laminate would be the same as if there were no thermal contribution ($\Delta T = 0$). Figures 4 and 5 shows how the σ_{22} and τ_{12} stresses vary between a $\Delta T = -156°C$ (-280°F) and a $\Delta T = 0$. The $\Delta T = 0$ case also indicates that when θ is between 15 and 30 degrees, relatively high shear stresses are present along the fiber but the transverse normal stresses are compressive.

Finite Element Analysis

A quasi-3D finite element code [7] was used to calculate the in-plane and interlaminar stresses near the free edges of $(0/\theta/-\theta)_s$ laminates subjected to the same loading specified above. The model was constructed assuming a unit ply thickness, h, in a laminate whose total width was 40h. Figure 6 shows the region of the mesh, near the free edge, used to model a representative cross section of the laminate normal to the direction of the applied tensile load. Because of symmetry, only one quarter of the cross section was modeled. The model consisted of 108 eight-noded quadrilateral isoparametric elements having a total of 367 nodes, each with 3 degrees of freedom. The smallest element at the free edge was equal to one eighth of a ply thickness, corresponding to a distance of one sixteenth of a ply thickness between the node on the free edge and the nearest mid-side node. Because the graphite epoxy material being model has approximately 20 fibers through the thickness of a single ply, no attempt was made to refine the mesh further because the size of the element used was on the same order as the fiber diameter. If the mesh were to be further refined, the assumption that the material was a homogeneous anisotropic continuum would no longer be valid.

The in-plane stresses in the central $-\theta$ degree plies were calculated at nodes along the midplane of the laminate thickness. These in-plane stresses were transformed into the lamina coordinate system, and the stresses normal to the fiber direction, σ_{22}, and the shear stresses along the fiber direction, τ_{12}, were plotted in the vicinity of the straight free edge. These stress distributions were used to obtain a qualitative assessment of the stresses responsible for matrix cracking in the off-axis plies.

In-plane Normal Stresses

Figure 7 shows the distribution across the laminate width of the in-plane normal stress, σ_{22}, for $(0/\theta/-\theta)_s$ graphite laminates

subjected to a total (mechanical + thermal) axial strain of 0.01, assuming a ΔT of -156°C (-280°F), where θ = 15, 30, and 45 degrees. The values in the interior, corresponding to (b-y)/h = 5, agree with the values calculated from laminated plate theory (fig. 3), where the normal stresses in the 45 degree case are in tension and the normal stresses in the 15 and 30 degree cases are in compression. However, near the free edge, (b-y)/h = 0, the magnitude of the tensile stresses increases for the 45 degree case and the sign of the normal stresses change from compression to tension for the 15 and 30 degree cases. The results for the 15 and 30 degree cases were expected to bound the results for the 20 and 25 degree cases, and hence, these layups were not analyzed.

The reversal in sign of the transverse normal stresses for the 15 and 30 degree cases is not limited to the particular applied loading shown in figure 7. For example, figure 8 shows the distribution across the laminate width of the in-plane normal stress, σ_{22}, for a $(0/15/-15)_s$ laminate subjected to total axial strains of 0.005 and 0.01 and a ΔT of -156°C (-280°F). Figure 9 shows the distribution across the laminate width of the in-plane normal stress, σ_{22}, for a $(0/15/-15)_s$ laminate subjected to a total axial strains of 0.01 with a ΔT = -156°C (-280°F) and a ΔT = 0. In both figures 8 and 9, the transverse normal stress is also compressive in the interior of the laminate width and becomes tensile at the free edge.

In-plane Shear Stresses

Figure 10 shows the distribution across the laminate width of the in-plane shear stress, τ_{12}, for θ = 15, 30, and 45 degrees. The values in the interior, corresponding to (b-y)/h = 5, agree with the values calculated by laminated plate theory (fig.3). In the interior of the laminate width, the 30 degree case has the largest shear stresses, and the 15 degree case has the lowest shear stresses. However, near the free edge, (b-y)/h = 0, the magnitudes of these shear stresses change. Near the free edge, the 15 degree case has larger shear stresses than the 30 and 45 degree cases.

The change in the magnitude of the in-plane shear stresses is not limited to the particular applied loading shown in figure 10. For example, figure 11 shows the distribution across the laminate width of the in-plane shear stress, τ_{12}, for a $(0/15/-15)_s$ laminate subjected to total axial strains of 0.005 and 0.01 and a ΔT of -156°C (-280°F). Figure 12 shows the distribution across the laminate

width of the in-plane shear stress, τ_{12}, for a $(0/15/-15)_s$ laminate subjected to a total axial strains of 0.01 with a ΔT = -156°C (-280°F) and a ΔT = 0. In both figures 11 and 12, the magnitude of the in-plane shear stress at the free edge is greater than the magnitude in the interior of the laminate width.

Interlaminar Stresses

Figure 13 shows the interlaminar normal stress, σ_{zz}, and the interlaminar shear stress, τ_{xz} and τ_{yz}, distributions across the laminate width in the 15/-15 interface of a $(0/15/-15)_s$ graphite epoxy laminate. This analysis indicates that the magnitude of the interlaminar shear stress, τ_{xz}, is very high near the free edge, and that the interlaminar normal stress, σ_{zz}, is compressive. Other authors have obtained similar results, and have concluded that edge delaminations will form in the 15/-15 interfaces of these laminates due to the high interlaminar shear stress, τ_{xz} [8-10]. However, the results in figure 13 do not take into account the matrix cracking that may be present in the -15 degree plies.

The presence of matrix cracks will alter the interlaminar stress state at the free edge, resulting in a change in sign, from compression to tension, of the interlaminar normal stress, σ_{zz} [11]. For example, fig.14 shows the interlaminar normal stresses, calculated from a 3D finite element analysis, in the 15/-15 interfaces of a $(0/15/-15)_s$ graphite epoxy laminate at the intersection of the straight free edge and a matrix crack in the -15 degree ply. The σ_{zz} stresses near the free edge in the 15/-15 interface that were compressive before the introduction of the matrix crack (fig.13), become very large tensile stresses once the matrix crack is present. A similar reversal in σ_{zz} stresses was found in ref.[12] when 15 degree matrix cracks were modeled in $(15/90/-15)_s$ glass epoxy laminates.

DISCUSSION

The finite element results indicate that matrix cracks may initiate in the central $-\theta$ plies at the edge of the $(0/\theta/-\theta)_s$ laminates where the in-plane transverse tensile stresses exist and have their greatest magnitude. This is especially true for brittle epoxy matrix composites, such as AS4/3501-6, where the transverse tensile strength is typically on the order of one-half the shear strength. For

example, fig.15 compares the relative magnitudes of the interlaminar shear strength, τ_{13c}, measured using a short beam shear test [13], to the transverse tensile strength, σ_{22c}, measured using a 90 degree tension test [14], and the interlaminar tensile strength, σ_{33c}, measured using a 0 degree curved beam bending test [14]. The matrix dominated tensile strengths are approximately one half of the interlaminar shear strength for AS4/3501-6.

The analytical results indicate that the use of in-plane stresses calculated from laminated plate theory to predict the onset of matrix cracking, often referred to as "first ply failure" in phenomenological failure criteria, may be unconservative because these laminate theory stresses represent minimum values in the interior of the laminate. The first "failure" of a ply, however, occurs near the free edge (fig.1) where in-plane transverse tensile stresses exist and have their greatest magnitude (fig.7).

The presence of matrix cracks will alter the interlaminar stress state at the free edge, resulting in a change in sign, from compression to tension, of the interlaminar normal stress, σ_{zz} [11]. Furthermore, these laminates do not delaminate uniformly along the length of the laminate near the free edges as typically observed for edge delamination [15-17]. Instead, the delaminations are localized and bounded by angle ply matrix cracks and the free edge, as shown in figures 1&2, and in fig.3 of ref.9. Hence, the local tensile interlaminar normal stresses near the free edge resulting from the formation of matrix cracks, in addition to the high interlaminar shear stresses that are present near the free edge, will contribute significantly to the formation of local delaminations in these laminates.

CONCLUSIONS

Quasi-static tension tests were conducted on AS4/3501-6 graphite epoxy $(0_2/\theta_2/-\theta_2)_s$ laminates, where θ was 15, 20, 25, and 30 degrees. Dye penetrant enhanced X-ray radiography was used to document the onset of matrix cracking in the central $-\theta$ degree plies and local delamination onset in the $\theta/-\theta$ interface at the intersection of the matrix cracks and the free edge.

A quasi-3D finite element analysis was conducted to calculate the stresses responsible for matrix cracking in the off-axis plies. In contrast to the results of laminated plate theory, which indicated that the transverse normal stresses were compressive, the finite element analysis yielded tensile transverse normal stresses near the free edge. Hence, the analytical results indicated that the use of in-plane stresses calculated from laminated plate theory to predict the onset of matrix cracking, often referred to as "first ply failure" in phenomenological failure criteria, may be unconservative because these laminate theory stresses represent minimum values in the interior of the laminate. The first "failure" of a ply, however, occurs near the free edge where in-plane transverse tensile stresses exist and have their greatest magnitude.

The presence of matrix cracks will alter the interlaminar stress state at the free edge, resulting in a change in sign, from compression to tension, of the interlaminar normal stress, σ_{zz} [11]. Furthermore, these laminates do not delaminate uniformly along the length of the laminate near the free edges as typically observed for edge delamination. Instead, the delaminations are localized and bounded by angle ply matrix cracks and the free edge. Hence, the local tensile interlaminar normal stresses near the free edge resulting from the formation of matrix cracks will contribute significantly to the formation of local delaminations in these laminates.

REFERENCES

1. Reifsnider, K.L., and Talug, A., "Analysis of Fatigue Damage in Composite Laminates," Int. J. of Fatigue, Vol.3,No.1, Jan.1980, pp.3-11.

2. Kress, G.R., and Stinchcomb, W.W., "Fatigue Response of Notched Graphite Epoxy Laminates," Recent Advances in Composites in the United States and Japan, ASTM STP 864, 1985, pp.173-196.

3. Murri,G.B., O'Brien,T.K., and Salpekar,S.A., "Tension Fatigue of Glass/Epoxy and Graphite/Epoxy Tapered Laminates," Proceedings of the 46th AHS Annual Forum, Vol.1, May 1990, pp.721-734 (Also in NASA TM 102628, April 1990).

4. O'Brien,T.K., Rigamonti,M., and Zanotti,C., "Tension Fatigue Analysis and Life Prediction for Composite Laminates," Int. J. of Fatigue, Vol.11,No.6, Nov.1989, pp.379-394.

5. O'Brien,T.K., and Raju,I.S., "Strain Energy Release Rate Analysis of Delamination Around an Open Hole in a Composite Laminate," 25th AIAA Structures, Dynamics, and Materials Conference, Palm Springs, Proceedings, May 1984, AIAA-84-0961, pp.526-536.

6. Jones,R.M., Mechanics of Composite Materials, McGraw Hill, Washington, D.C., 1975.

7. Raju,I.S., "Q3DG - A computer program for Strain Energy Release Rates for Delamination Growth in Composite Laminates," NASA CR 178205, Nov. 1986.

8. Soni,S.R., and Kim,R.Y., "Delamination of Composite Laminates Stimulated by Interlaminar Shear," Composite Materials:Testing and Design, Seventh Conference, ASTM STP 893, 1986, pp.286-307.

9. Lagace,P.A., and Brewer,J.C., "Studies of Delamination Growth and Final Failure under Tensile Loading," ICCM VI, London, Vol.5, Proceedings, July 1987, pp.262-273.

10. Brewer,J.C., and Lagace,P.A., "Quadratic Stress Criterion for Initiation of Delamination," J. of Composite Materials, Vol.22, No.4, December 1988, pp.1141-1155.

11. Salpekar,S.A., and O'Brien,T.K., "Analysis of Matrix cracking and Local Delamination in $(0/\theta/-\theta)_S$ Graphite Epoxy Laminates under Tension Load," ICCM VIII, Honolulu, Proceedings, July, 1991.

12. Fish,J.C., and O'Brien,T.K., "Three-Dimensional Finite Element Analysis of Delamination from Matrix Cracks in Glass-Epoxy Laminates," Composite Materials: Testing and Design, 10th Volume, ASTM STP 1120, 1992.

13. Sun, C.T., and Kelly, S.R., "Failure in Composite Angle Structures, Part:I, Initial Failure," J. of Reinforced Plastics and Composites, Vol.7, May 1988, pp.220-232.

14. Martin,R.H., and Jackson,W.C., "Damage Prediction in Curved Composite Laminates," to be presented at the Fourth ASTM Symposium on Composite Materials: Fatigue and Fracture, Indianapolis, Indiana, May, 1991.

15. O'Brien,T.K., Johnston,N.J., Raju,I.S., and Morris,D.H., "Comparisons of Various Configurations of the Edge Delamination Test for Interlaminar Fracture Toughness," Toughened Composites, ASTM STP 937, 1987, pp.199-221.

16. O'Brien,T.K., "Characterization of Delamination Onset and Growth in a Composite Laminate," Damage in Composite Materials, ASTM STP 775, 1982, pp.140-167.

17. O'Brien,T.K., "Mixed-mode Strain Energy Release Rate Effects on Edge Delamination of Composites," Effects of Defects in Composite Materials, ASTM STP 836, 1984, pp.125-142.

TABLE 1

$(0_2/\theta_2/-\theta_2)_s$ AS4/3501-6 GRAPHITE EPOXY
LAMINA PROPERTIES

E_{11} = 135 GPa (19.5 x 10^6 Psi)

E_{22} = 11 GPa (1.6 x 10^6 Psi)

G_{12} = 5.8 GPa (0.847 x 10^6 Psi)

ν_{12} = 0.301

α_1 = -0.41 x10^{-6} /°C (-0.23 x10^{-6} /°F)

α_2 = 26.8 x10^{-6} /°C (14.9 x10^{-6} /°F)

Fig. 1a. RADIOGRAPH OF $(0_2/15_2/-15_2)_s$ LAMINATE AFTER ONSET OF DAMAGE

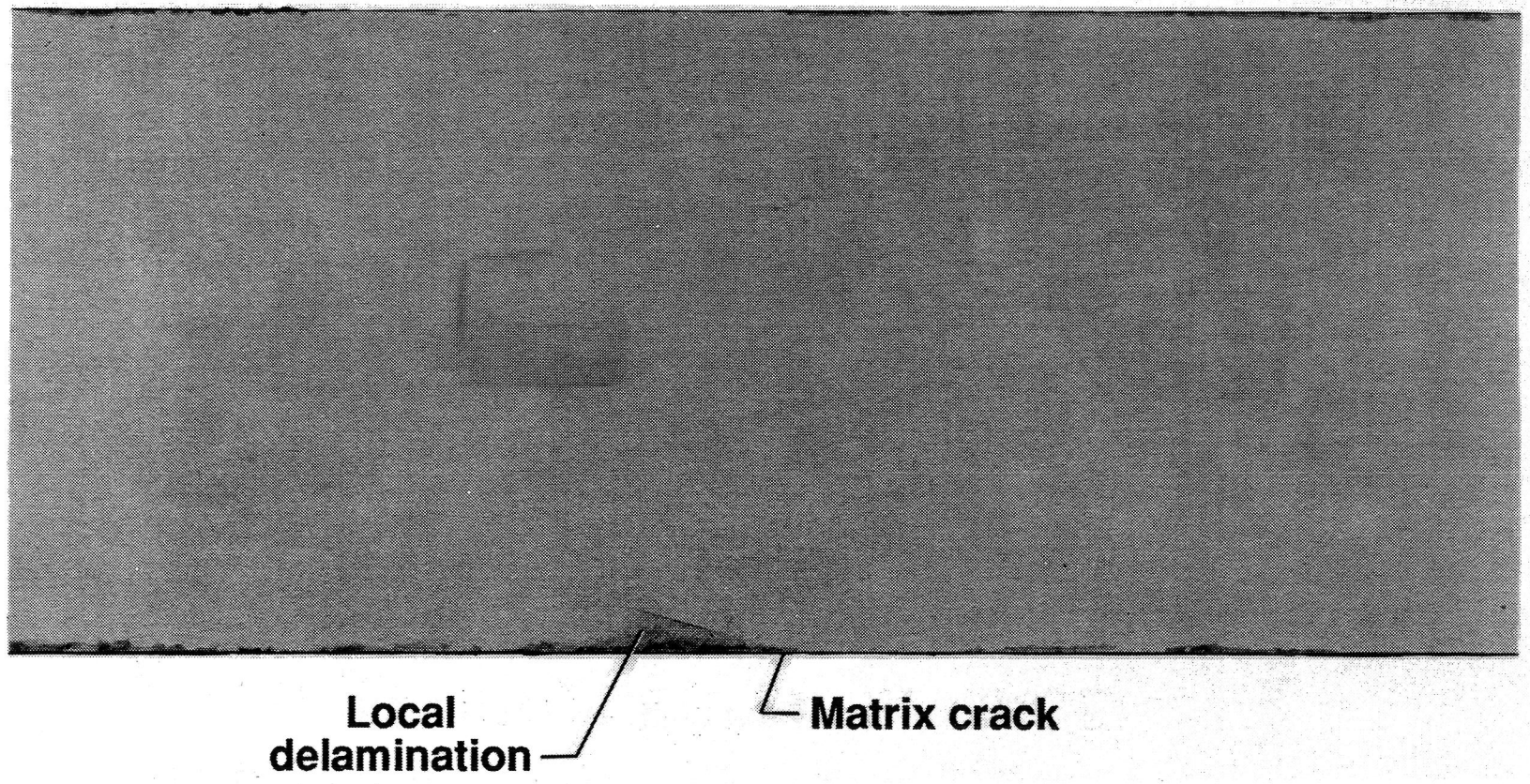

Fig. 1b. RADIOGRAPH OF $(0_2/20_2/-20_2)_s$ LAMINATE AFTER ONSET OF DAMAGE

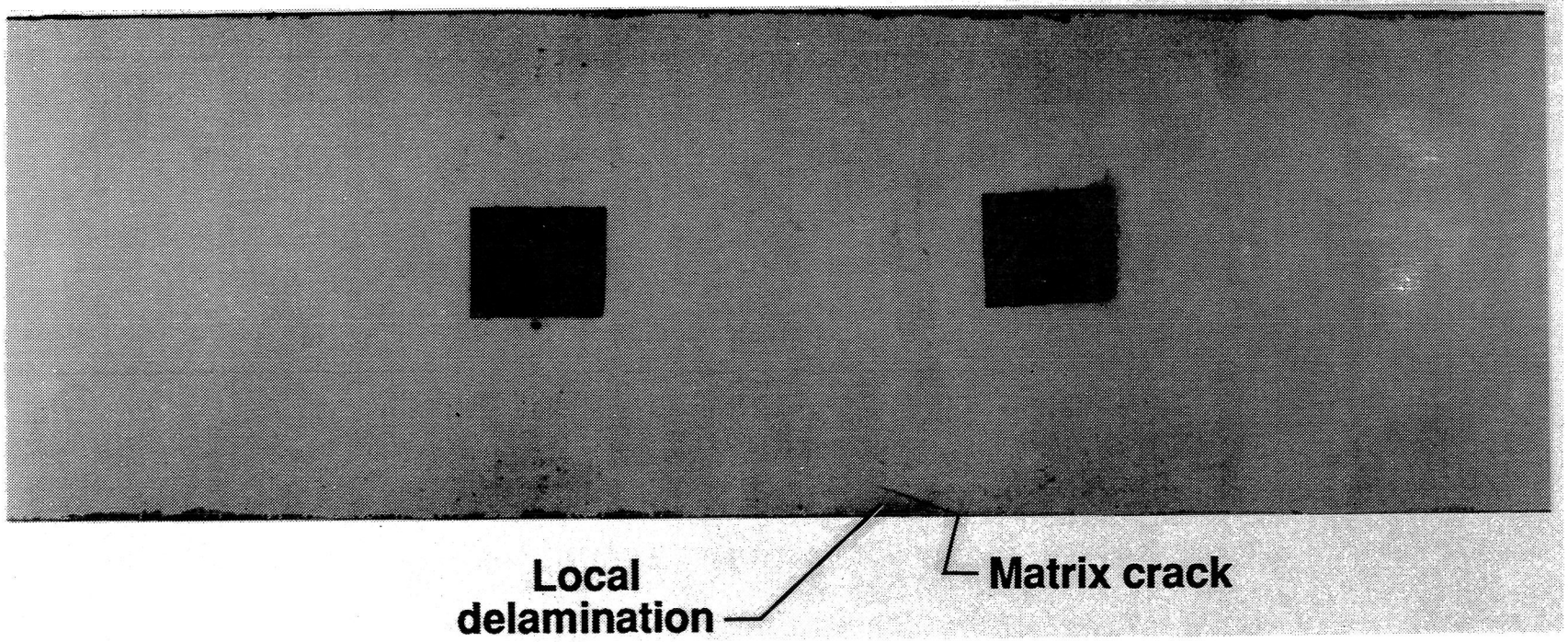

Fig. 1c. RADIOGRAPH OF $(0_2/25_2/-25_2)_s$ LAMINATE AFTER ONSET OF DAMAGE

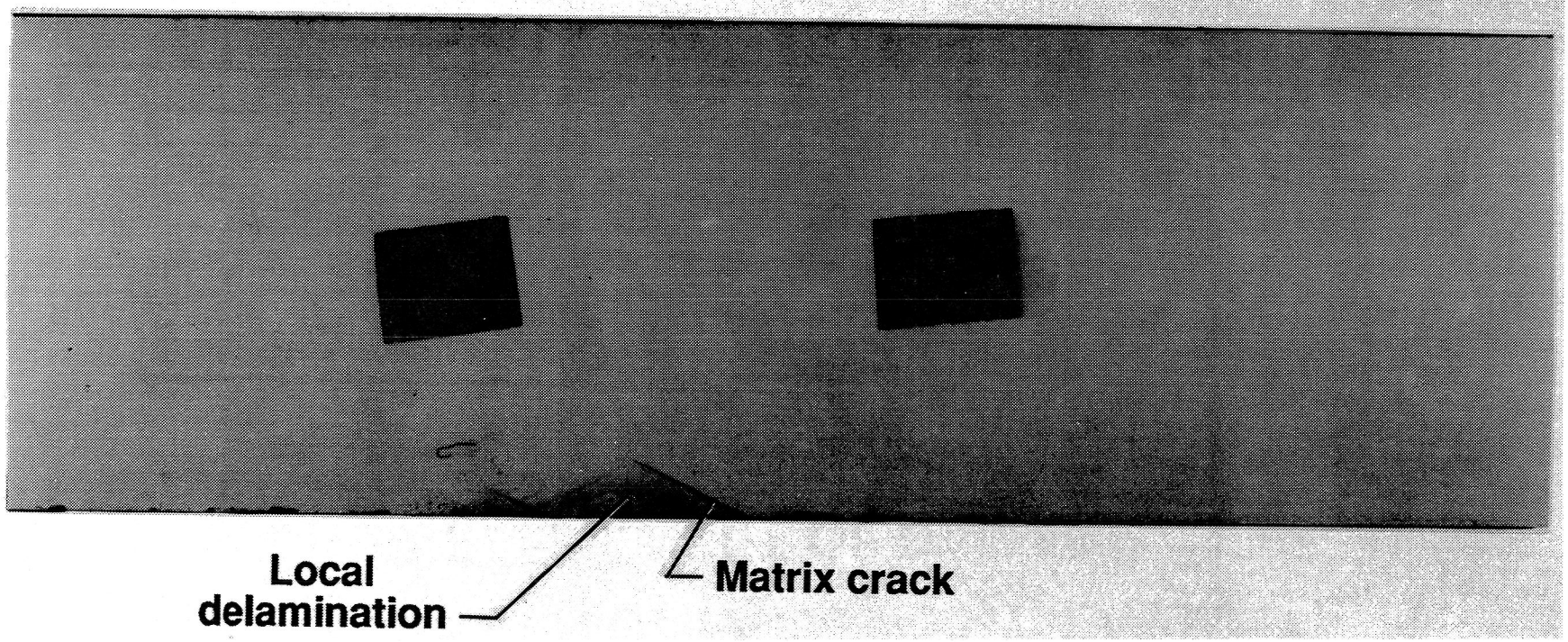

Fig. 1d. RADIOGRAPH OF $(0_2/30_2/-30_2)_s$ LAMINATE AFTER ONSET OF DAMAGE

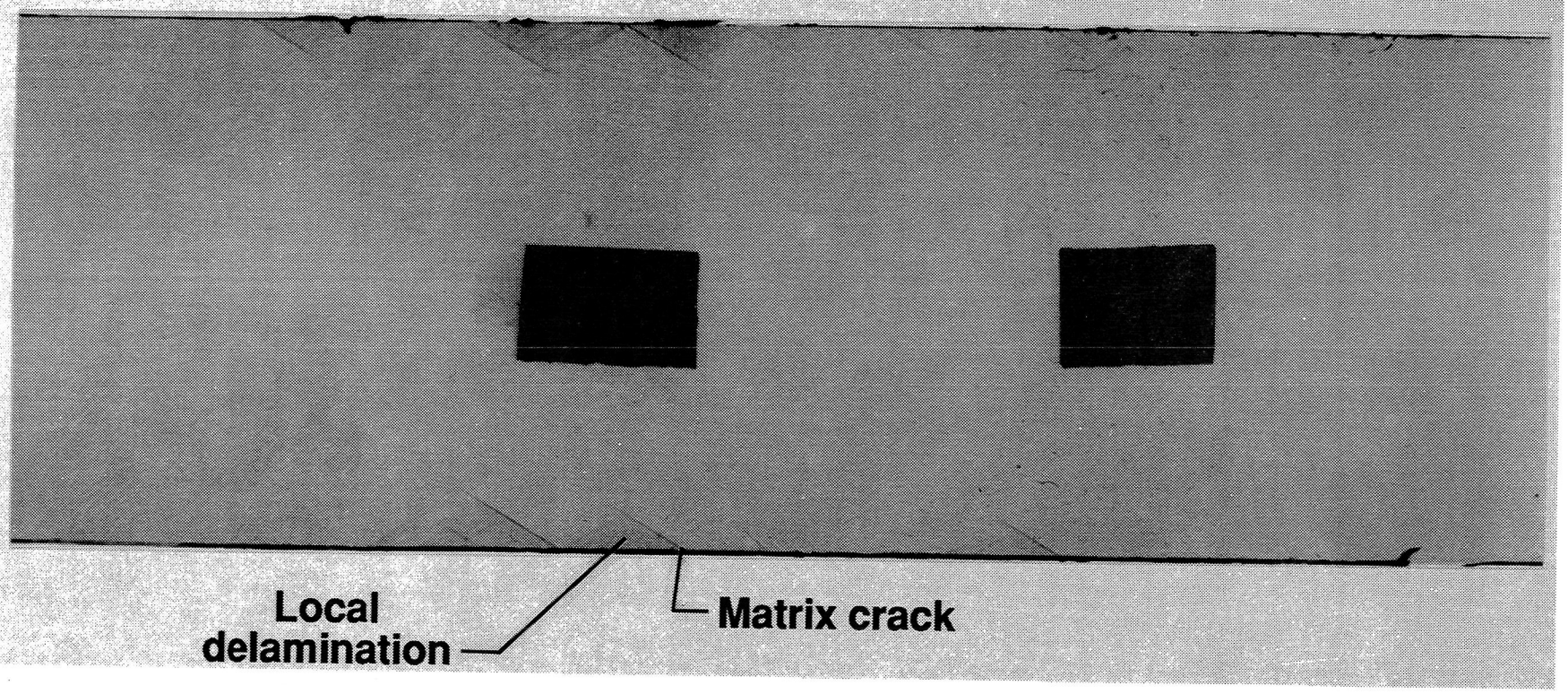

Fig. 2a. EDGE MICROGRAPHS OF $(0_2/\theta_2/-\theta_2)_s$ AS4/3501-6 LAMINATES

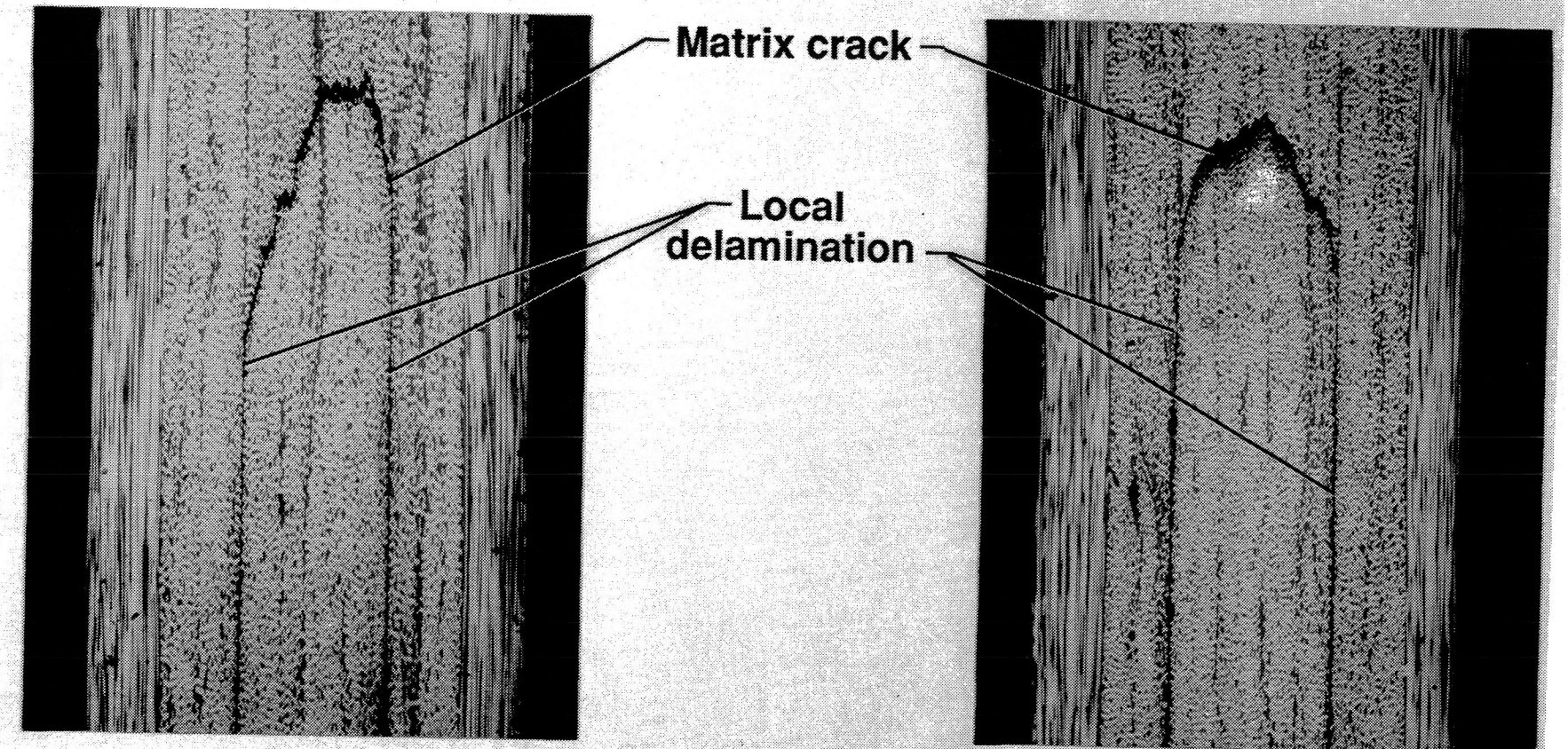

Fig. 2b. EDGE MICROGRAPHS OF $(0_2/\theta_2/-\theta_2)_s$ AS4/3501-6 LAMINATES

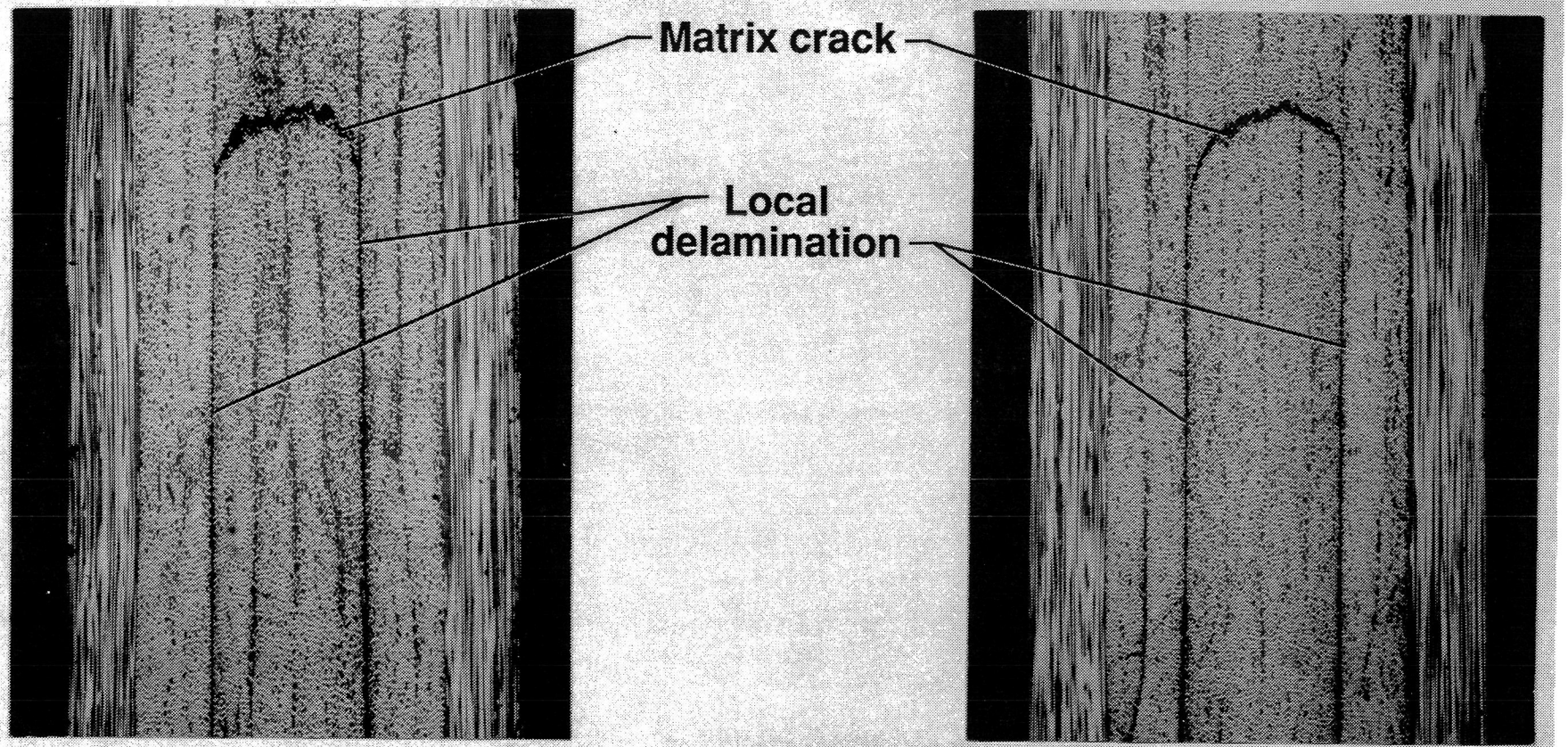

FIG.3 STRESSES IN -θ PLY OF $(0/\theta/-\theta)_s$ LAMINATES FROM LAMINATED PLATE THEORY (LPT)

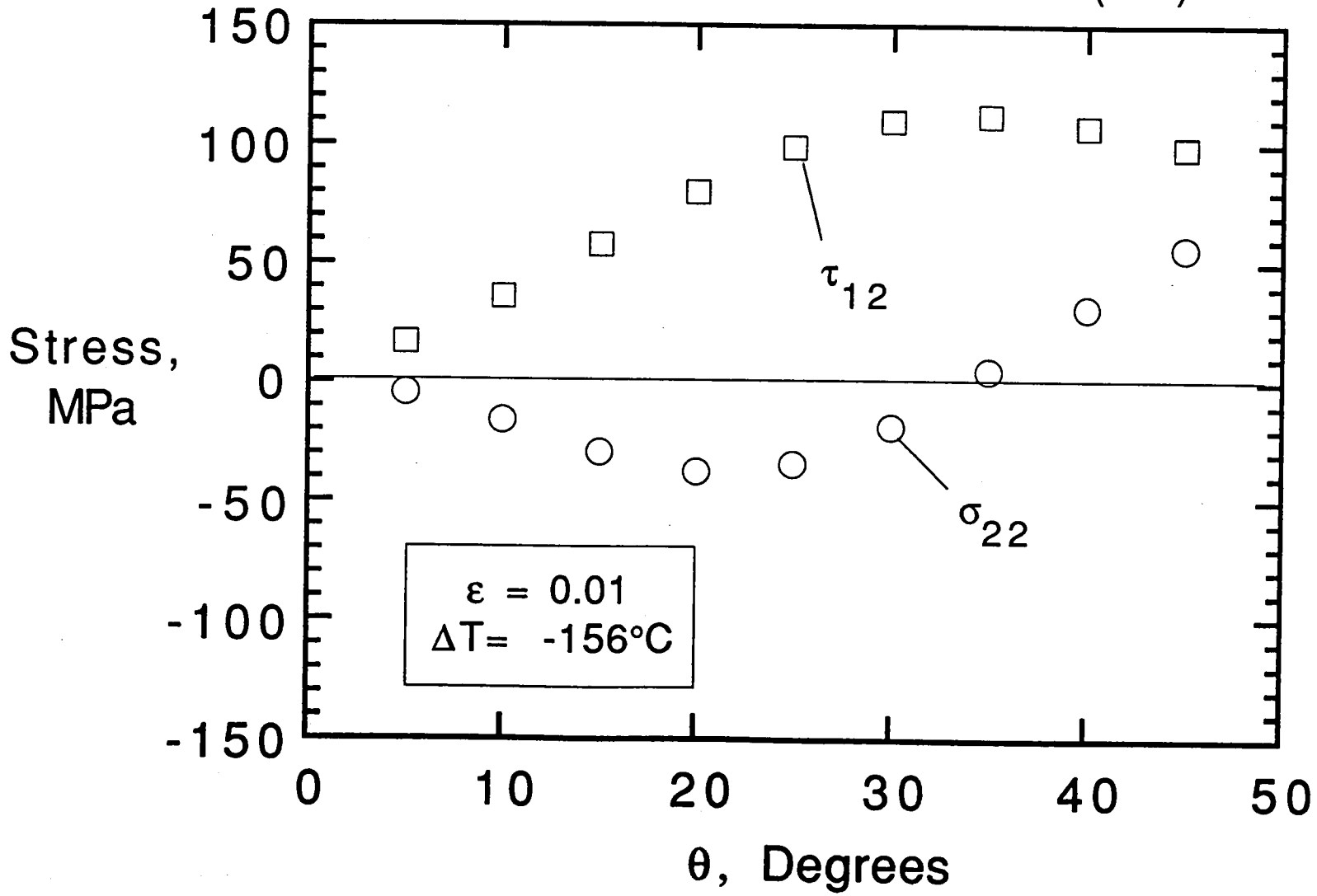

FIG.4 LAMINA NORMAL STRESSES IN -θ PLY OF
(0 /θ/ -θ)$_s$ LAMINATES FROM LPT

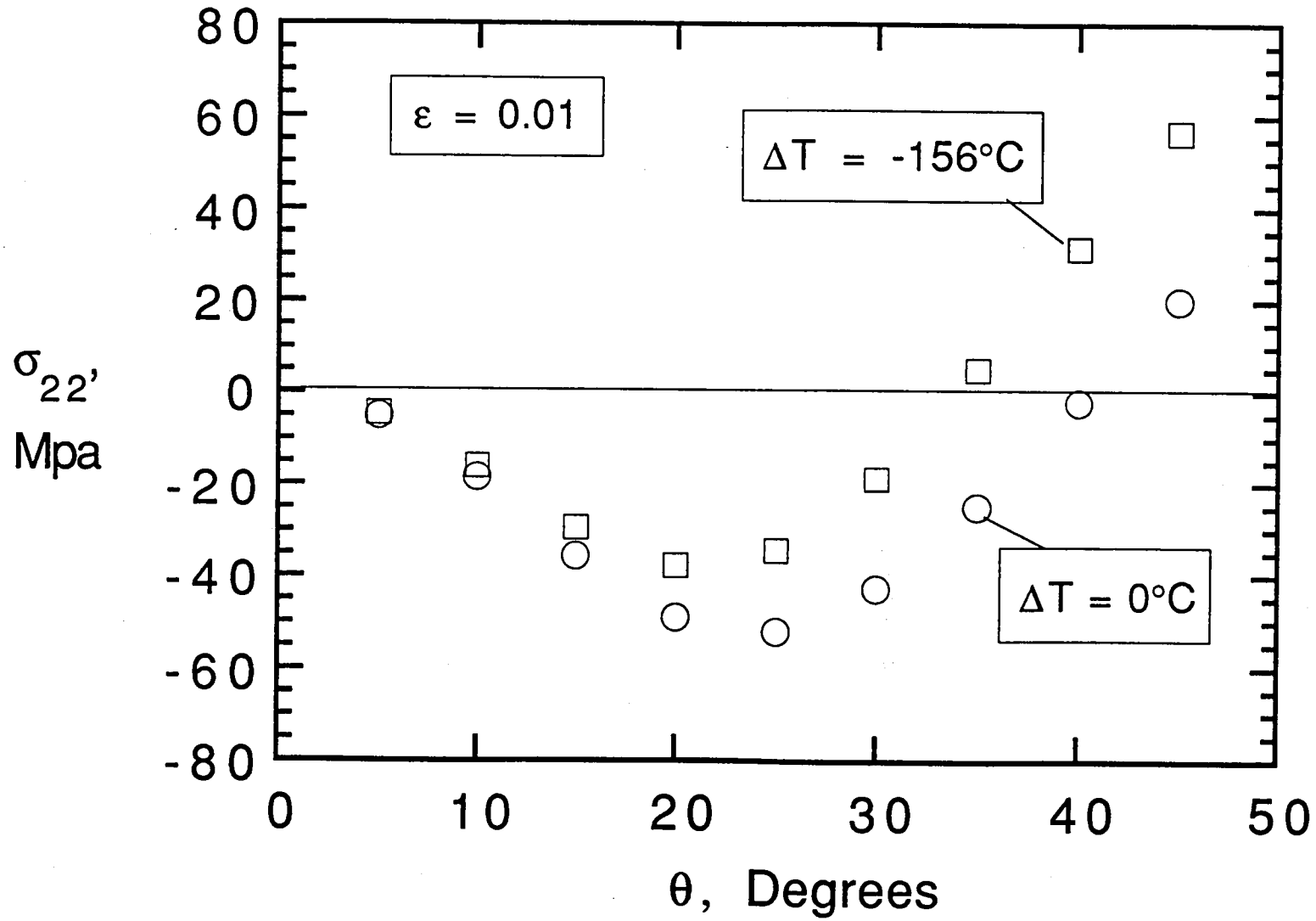

FIG.5 LAMINA SHEAR STRESSES IN -θ PLY OF
(0 /θ/ -θ)$_s$ LAMINATES FROM LPT

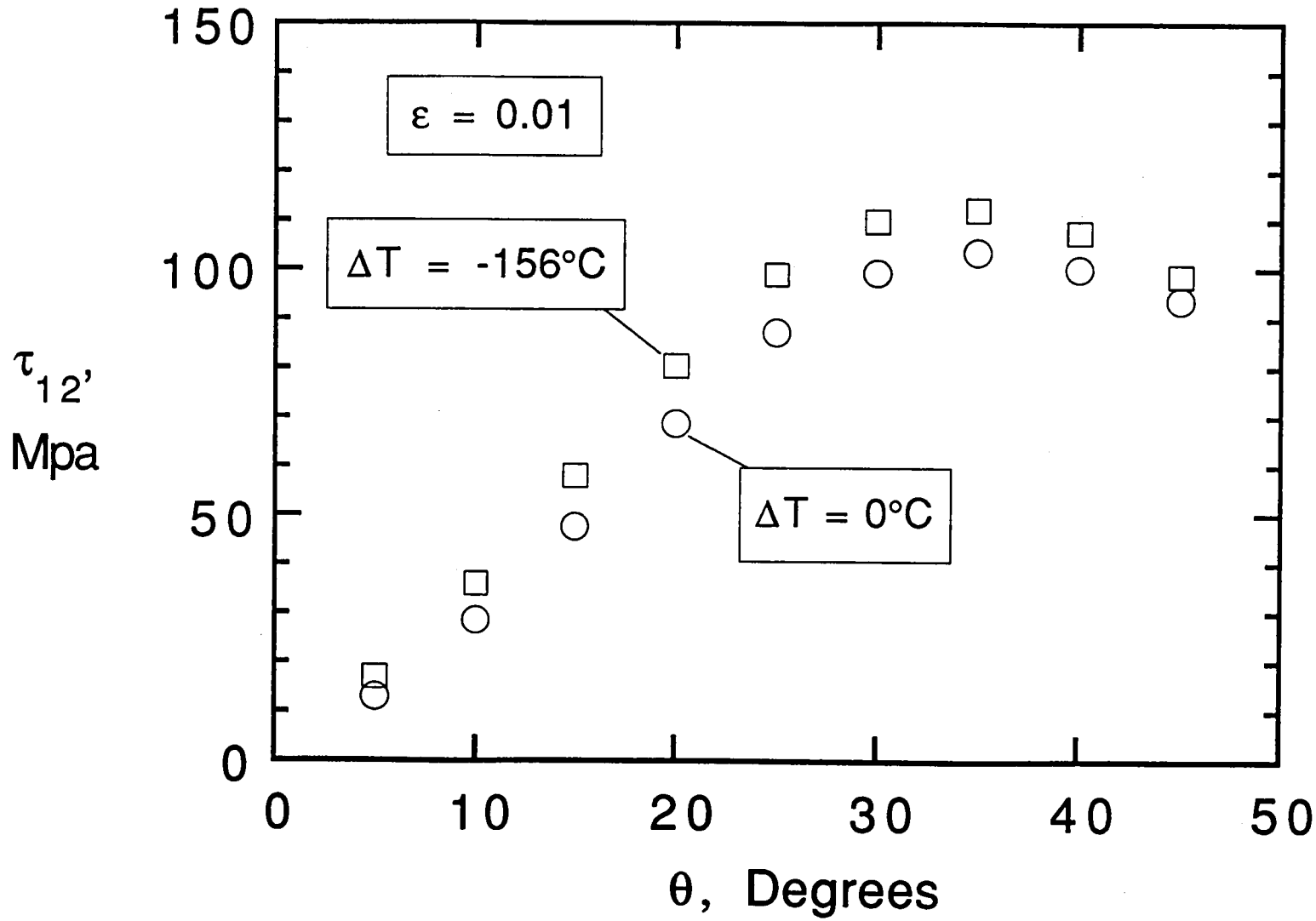

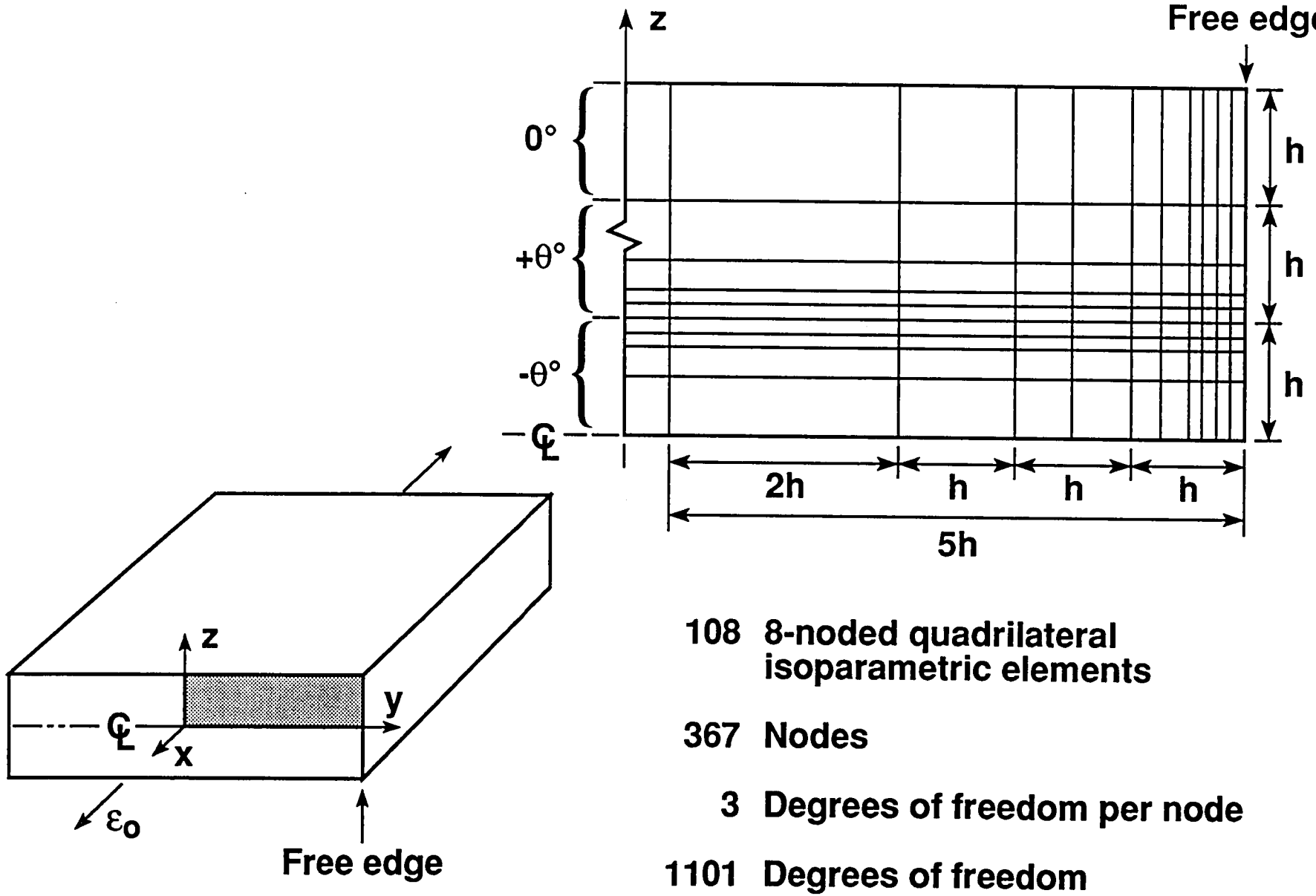

Figure 6. Quasi-3D finite element mesh near the free edge of a $(0/\theta/-\theta)_s$ laminate.

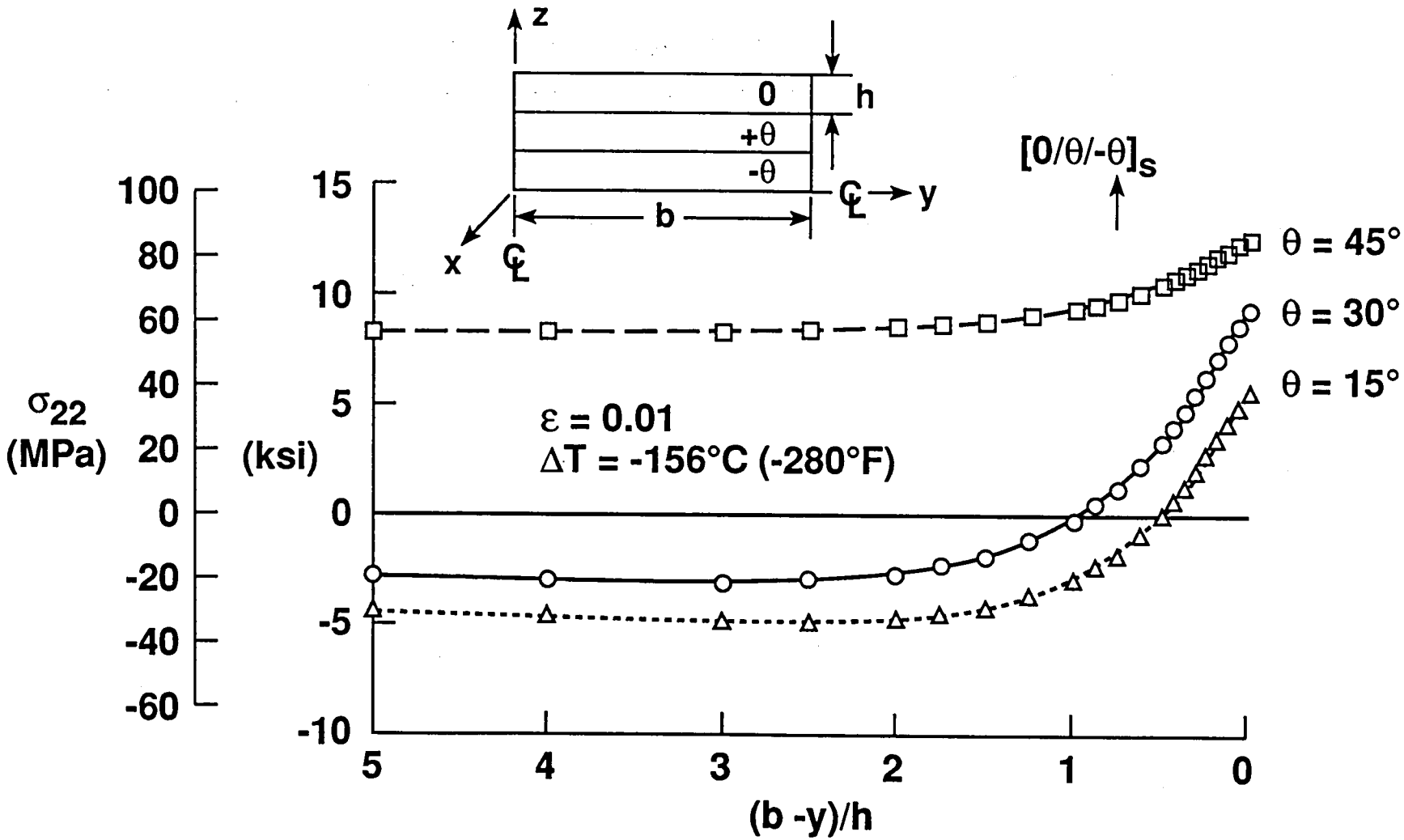

Figure 7. In-plane normal stress near the free edge of the -θ degree ply in $[0/\theta/-\theta]_s$ graphite epoxy laminate.

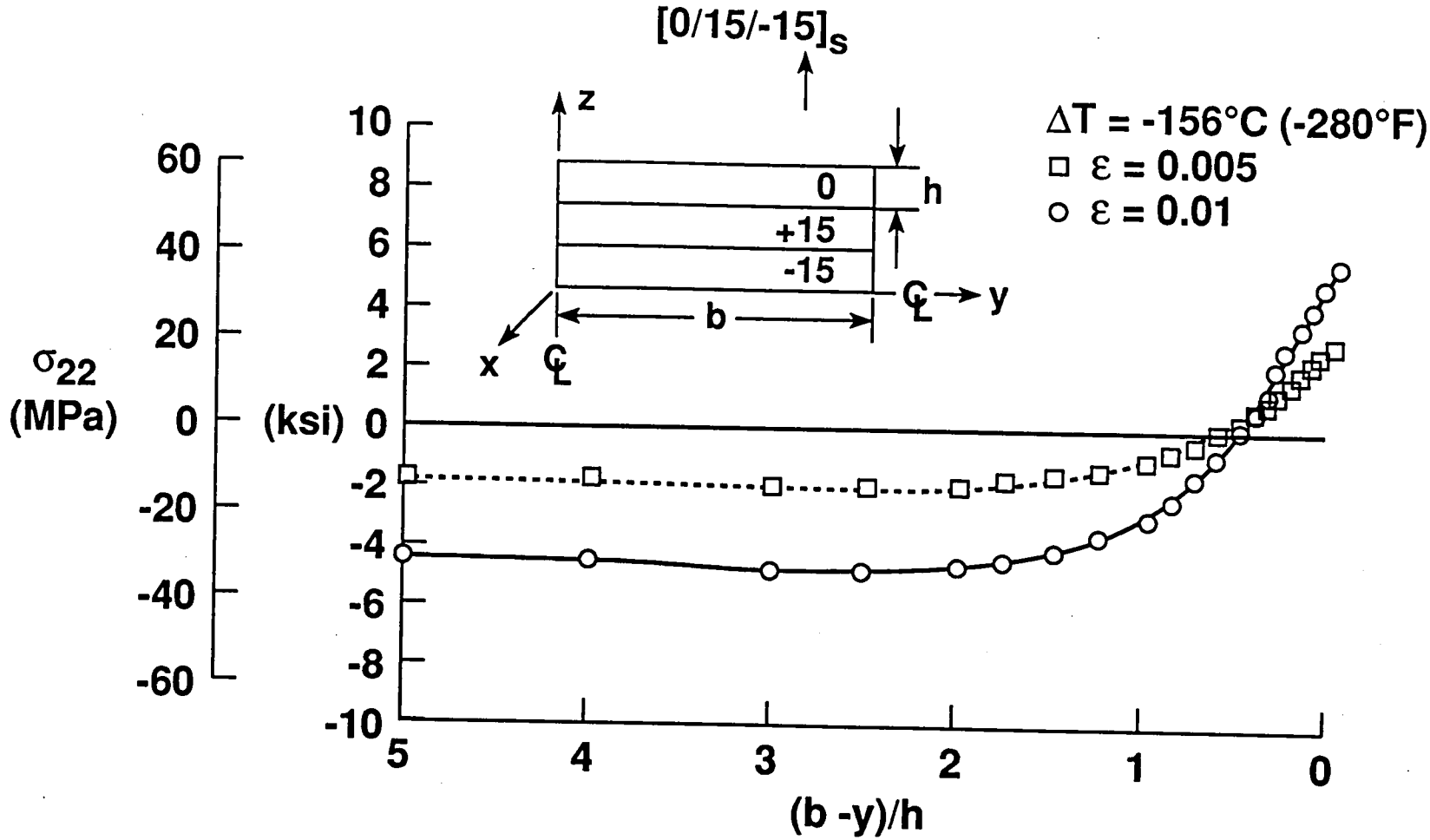

Figure 8. In-plane normal stress near the free edge of the -15° ply in $[0/15/-15]_s$ graphite epoxy laminate.

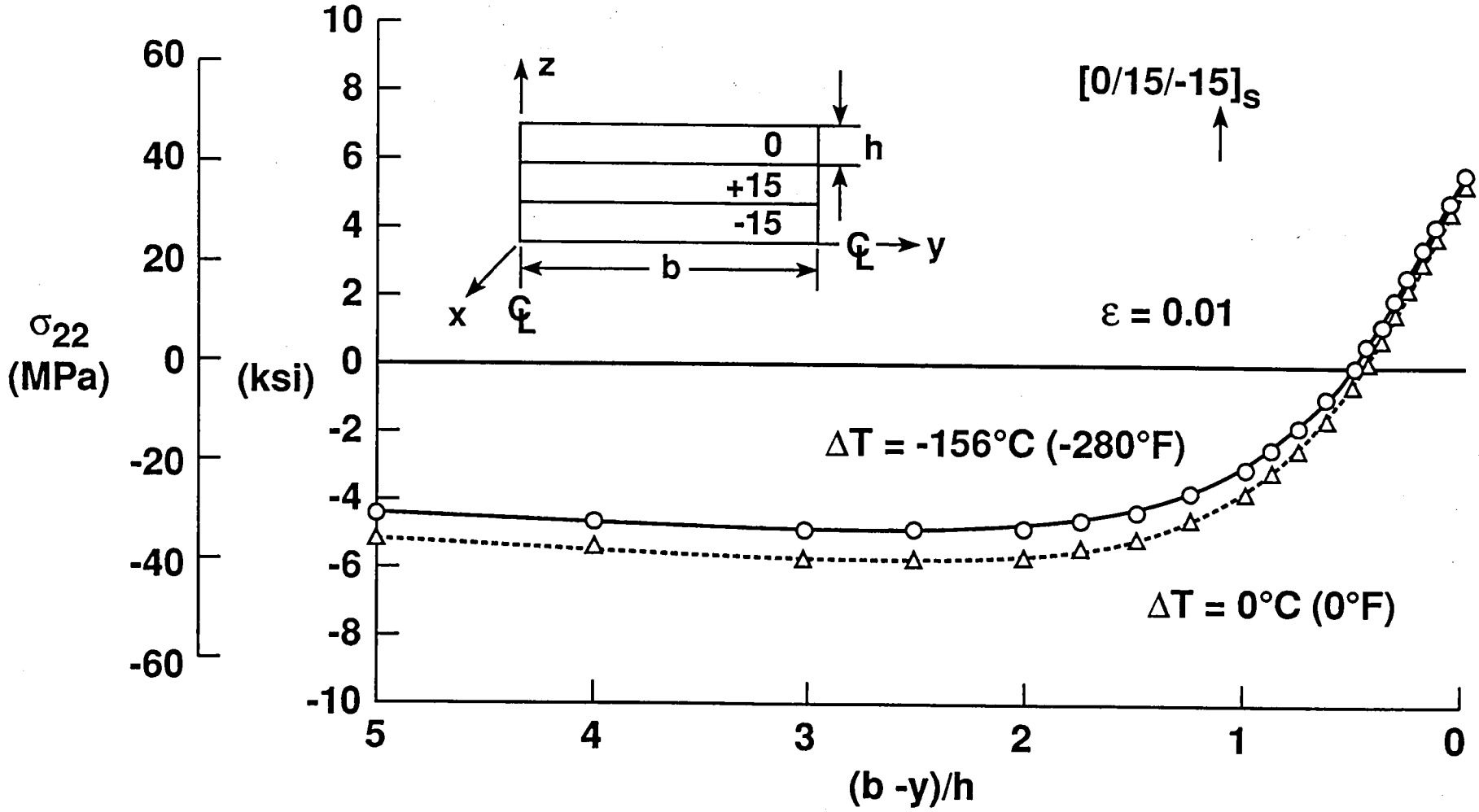

Figure 9. In-plane normal stress near the free edge of the -15° ply in $[0/15/-15]_s$ graphite epoxy laminate.

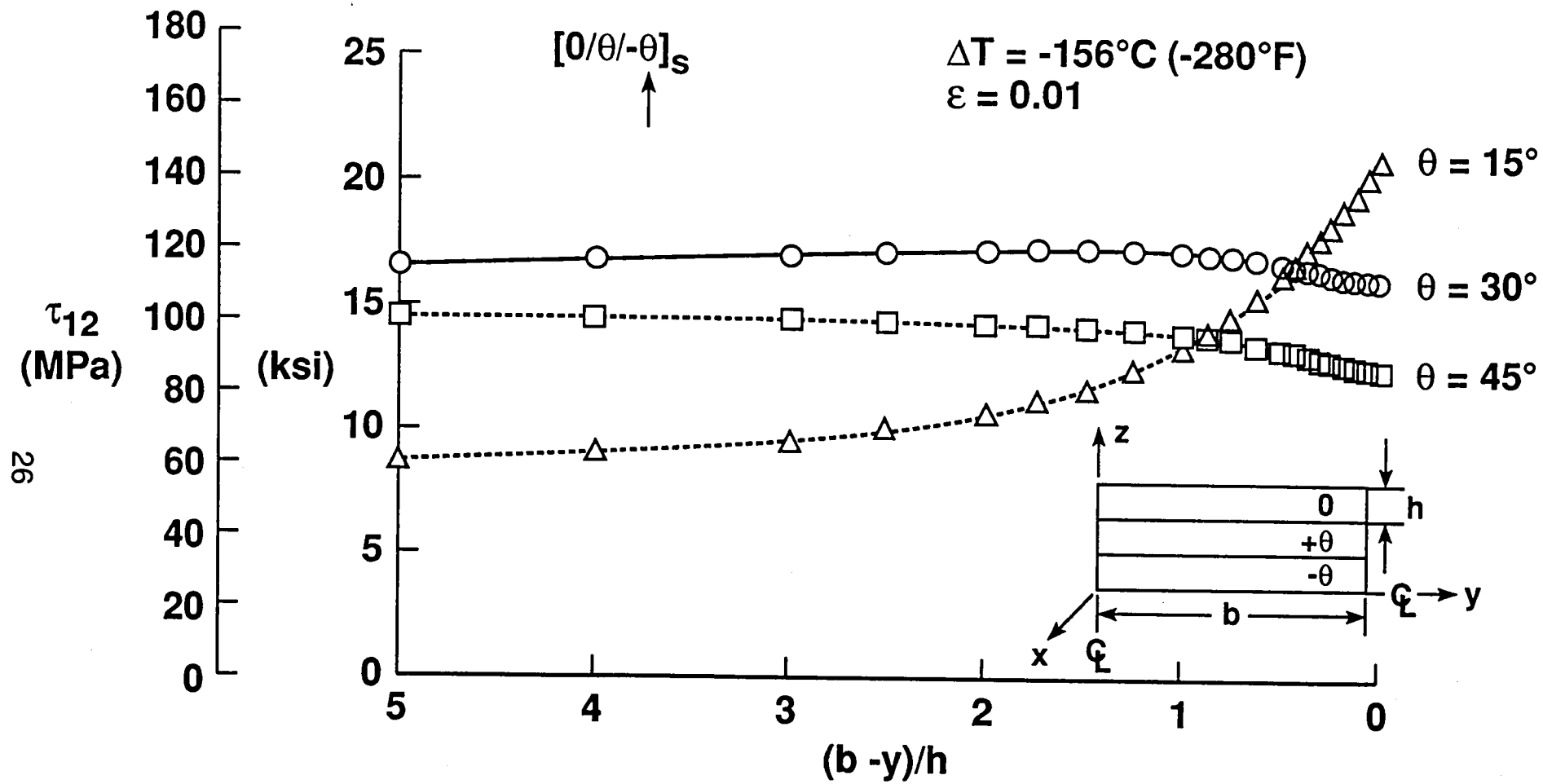

Figure 10. In-plane shear stress near the free edge of the -θ° ply in a $[0/\theta/-\theta]_s$ graphite epoxy laminate.

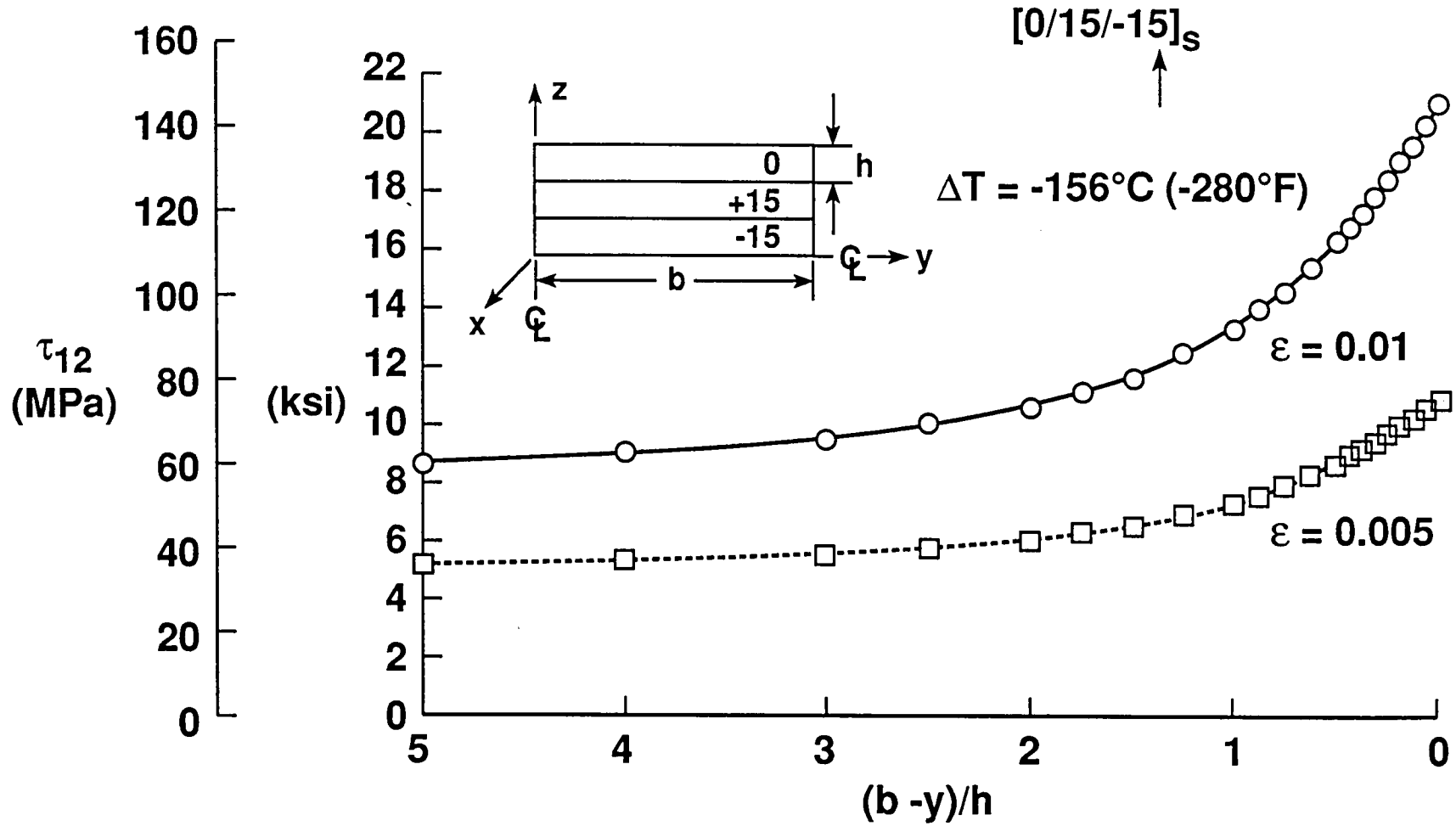

Figure 11. In-plane shear stress near the free edge of the -15° ply in a $[0/15/-15]_s$ graphite epoxy laminate.

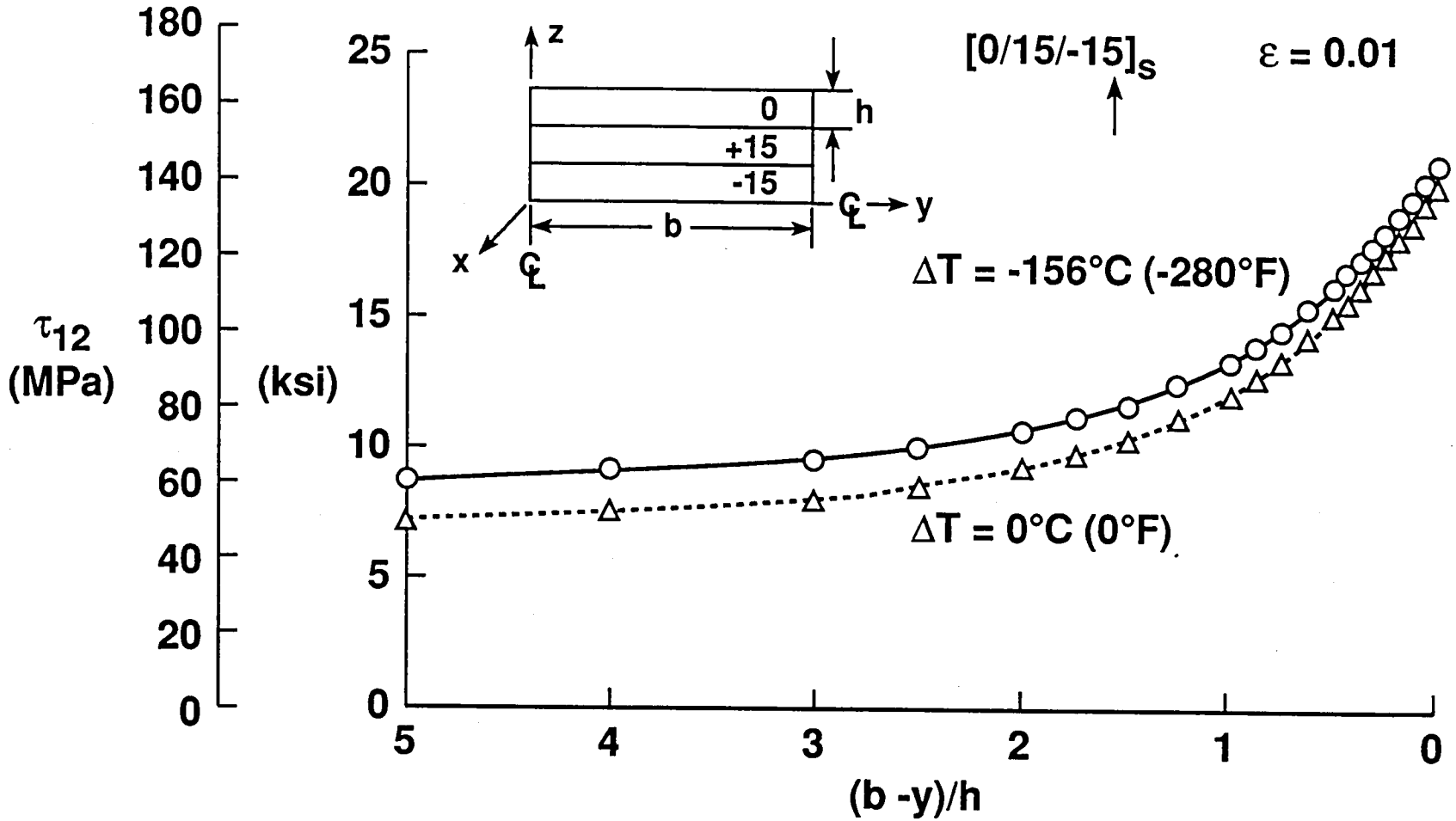

Figure 12. In-plane shear stress near the free edge of the -15° ply in a $[0/15/-15]_s$ graphite epoxy laminate.

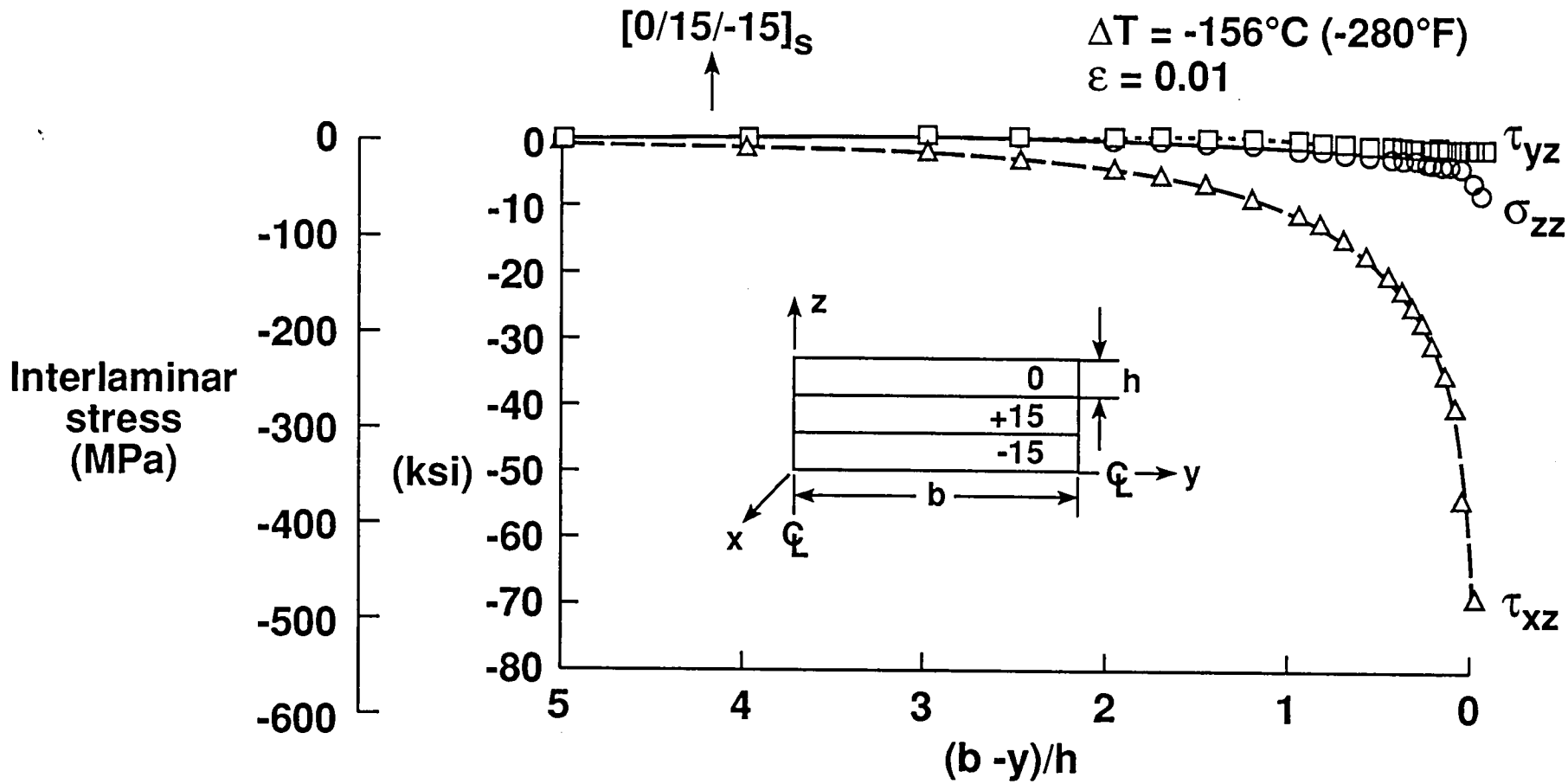

Figure 13. Interlaminar stresses near the free edge in the 15/-15 interface of a $[0/15/-15]_s$ graphite epoxy laminate.

Fig. 14.

NORMALIZED INTERLAMINAR NORMAL STRESS IN 15/-15 INTERFACE DUE TO MATRIX CRACK IN -15 PLY OF $(0/15/-15)_s$ LAMINATE

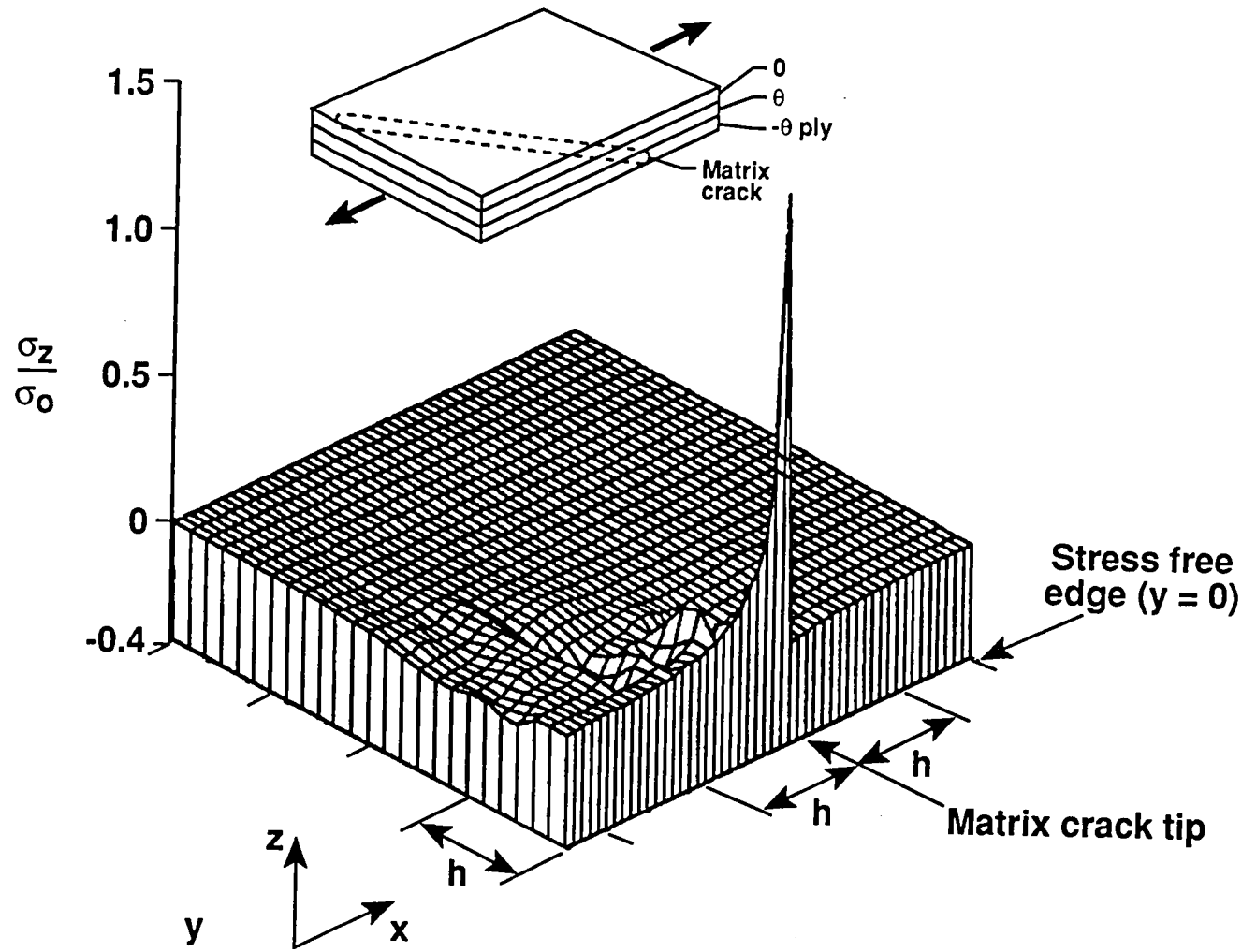

FIG.15 Matrix Dominated Strength Properties
AS4/3501-6 Graphite Epoxy

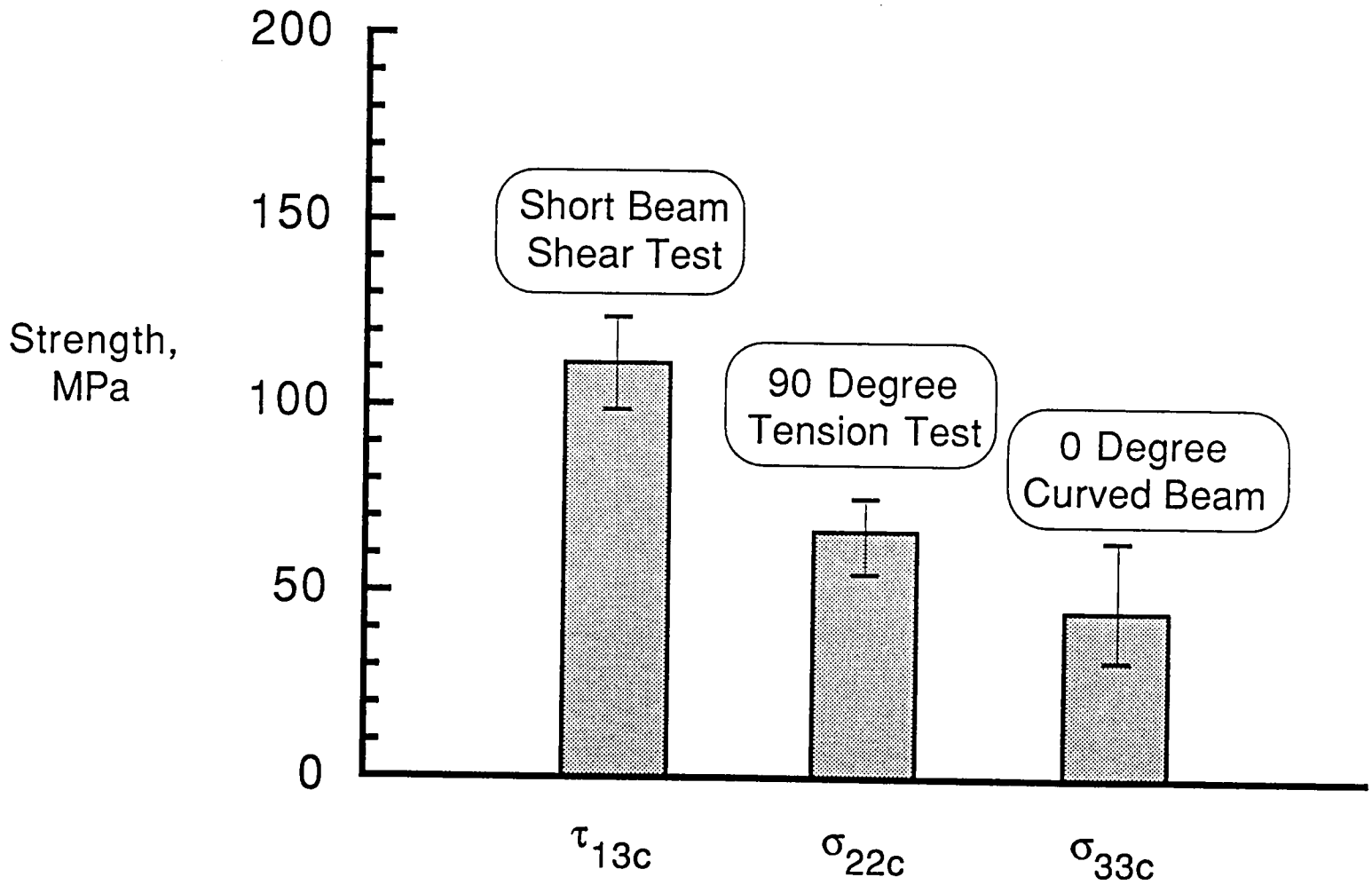

NASA

Report Documentation Page

1. Report No.	2. Government Accession No.	3. Recipient's Catalog No.
NASA TM-104055 AVSCOM TR-91-B-010		

4. Title and Subtitle	5. Report Date
Local Delamination in Laminates with Angle Ply Matrix Cracks: Part I Tension Tests and Stress Analysis	June 1991
	6. Performing Organization Code

7. Author(s)	8. Performing Organization Report No.
T. Kevin O'Brien and S. J. Hooper*	
	10. Work Unit No. 505-63-50-04

9. Performing Organization Name and Address	11. Contract or Grant No.
NASA Langley Research Center, Hampton, VA 23665-5225 U.S. Army Aviation Research and Technology Activity (AVSCOM) Aerostructures Directorate Hampton, VA 23665-5225	
	13. Type of Report and Period Covered
12. Sponsoring Agency Name and Address National Aeronautics and Space Administration Washington, DC 20546-0001 U.S. Army Aviation Systems Command St. Louis, MO 63166	Technical Memorandum
	14. Sponsoring Agency Code

15. Supplementary Notes

*Wichita State University
Wichita, Kansas

16. Abstract

Quasi-static tension tests were conducted on AS4/3501-6 graphite/epoxy $(0_2/\theta_2/-\theta_2)_s$ laminates, where θ was 15, 20, 25, or 30 degrees. Dye penetrant enhanced X-radiography was used to document the onset of matrix cracking in the central $-\theta$ degree plies and the onset of local delaminations in the $\theta/-\theta$ interface at the intersection of the matrix cracks and the free edge. Edge micrographs taken after the onset of damage were used to verify the location of the matrix cracks and local delaminations through the laminate thickness. A quasi-3D finite element analysis was conducted to calculate the stresses responsible for matrix cracking in the off-axis plies. Laminated plate theory indicated that the transverse normal stresses were compressive. However, the finite element analysis yielded tensile transverse normal stresses near the free edge. Matrix cracks formed in the off-axis plies near the free edge where in-plane transverse stresses were tensile and had their greatest magnitude. The influence of the matrix crack on interlaminar stresses is also discussed.

17. Key Words (Suggested by Author(s))	18. Distribution Statement
Composite material Graphite/epoxy Delamination Matrix crack	Unclassified - Unlimited Subject Category - 24

19. Security Classif. (of this report)	20. Security Classif. (of this page)	21. No. of pages	22. Price
Unclassified	Unclassified	32	A03